MITSUBISHI ELECTRIC RESEARCH LABORATORIES
http://www.merl.com

Secrecy Performance Analysis of Distributed Asynchronous Cyclic Delay Diversity-Based Cooperative Single Carrier Systems

Kim, Kyeong Jin; Liu, Hongwu; Wen, Maiwen; Orlik, Philip V.; Poor, H. Vincent

TR2020-084 July 01, 2020

Abstract

A joint data and interference transmission scheme based on a new distributed asynchronous cyclic delay diversity (dACDD) technique is proposed for cooperative communication systems. Without any perfect channel state information from a legitimate user (LU) and an eavesdropping user (EU), joint remote radio head (RRH) selection for the data and jamming signal transmissions is proposed for dACDD to achieve the maximum diversity gain at the LU, while degrading the receive signal-tointerference-plus-noise ratio at the EU. The proposed dACDD is the extension of distributed cyclic delay diversity, which requires a tight synchronization among the central control unit and RRHs. Thus, processing at each RRH causing no intersymbol interference at the LU is developed. Then, the selection scheme for a data RRH is proposed, which selects a single RRH connected with the channel having the greatest channel magnitude as the data RRH to transmit a desired confidential message and controls the remaining RRHs to transmit an artificial interference sequence to the LU and EU. For the proposed distributed system, the marginal secrecy outage probability and marginal probability of non-zero achievable secrecy rate are analyzed by deriving closed-form expressions, whose correctness is verified via link-level simulations over non-identically distributed frequency selective fading channels.

IEEE Transactions on Communications

Secrecy Performance Analysis of Distributed Asynchronous Cyclic Delay Diversity-Based Cooperative Single Carrier Systems

Kyeong Jin Kim, Hongwu Liu, Miaowen Wen, Philip V. Orlik, and H. Vincent Poor

***Abstract*—A joint data and interference transmission scheme based on a new distributed asynchronous cyclic delay diversity (dACDD) technique is proposed for cooperative communication systems. Without any perfect channel state information from a legitimate user (LU) and an eavesdropping user (EU), joint remote radio head (RRH) selection for the data and jamming signal transmissions is proposed for dACDD to achieve the maximum diversity gain at the LU, while degrading the receive signal-to-interference-plus-noise ratio at the EU. The proposed dACDD is the extension of distributed cyclic delay diversity, which requires a tight synchronization among the central control unit and RRHs. Thus, processing at each RRH causing no intersymbol interference at the LU is developed. Then, the selection scheme for a *data* RRH is proposed, which selects a single RRH connected with the channel having the greatest channel magnitude as the data RRH to transmit a desired confidential message and controls the remaining RRHs to transmit an artificial interference sequence to the LU and EU. For the proposed distributed system, the marginal secrecy outage probability and marginal probability of non-zero achievable secrecy rate are analyzed by deriving closed-form expressions, whose correctness is verified via link-level simulations over non-identically distributed frequency selective fading channels.**

***Index Terms*—Asynchronous distributed cyclic delay diversity, cyclic-prefixed single carrier system, physical layer security, secrecy outage probability, probability of non-zero achievable secrecy rate.**

I. Introduction

With wide deployment of various wireless technologies and rapid proliferation of their devices, maintaining a high degree of secure transmissions becomes a challenging task due to the open nature of wireless communications. Physical layer security (PLS) is emerging as a promising approach that enhances the secrecy level of wireless communications by utilizing physical characteristics of wireless channels, and has attracted considerable recent attention [2]–[7].

As one approach to PLS, the transmitting side jams an eavesdropping user (EU) by transmitting artificial noise (AN) [2], [8]–[13], with an objective degrading the reception quality at the EU while minimizing its degradation at a legitimate user (LU). When perfect channel state information (CSI) of the entire system, that is, for the legitimate channels and eavesdropper channels, is available at the transmitting side, secrecy beamforming can be used for joint data and jamming transmissions. The joint transmissions can emanate from either the same transmitter [8], [13]–[15] or separate transmitters [10], [11], [16], [17]. Similarly, multiple transmitters can be jointly used for joint data and jamming transmissions without utilizing secrecy beamforming [12]. A game theoretic approach was also proposed in [18], which optimized the secrecy performance of wireless networks with selfish jamming.

To jointly exploit the maximum achievable diversity gain from the frequency selective fading channels and multiuser diversity from cooperative transmissions, a cyclic-prefixed single carrier (CP-SC) transmission technique has been applied in several PLS systems such as [4] and [6]. For the first time, the authors of [4] verified that the multipath and multiuser diversity gains can be achieved by cooperative communications over frequency selective fading channels. Without specific descriptions, most of the existing works assume that perfect CSI for the legitimate channels is available by an explicit feedback [19] made by the LU. However, the EU can intercept this explicit feedback to lessen the effectiveness of PLS. Thus, it is desirable to avoid this explicit feedback type from PLS perspective. For this reason, an original distributed cyclic delay diversity (dCDD) scheme [20] proposed for non-PLS systems[1] has been adapted to distributed CP-SC systems that apply PLS in the presence of a single EU. With CSI for the eavesdropper channels, which is available by an active EU, joint selection for the data and jamming transmitters was proposed in [12]. In contrast to other works [10], [11], [13], [14], [16], [17], [22], transmit diversity and intersymbol interference (ISI)-free CP-SC transmissions are jointly exploited to degrade the reception quality, namely the signal-to-interference-plus-noise ratio (SINR), at the EU, while maximizing it, namely the signal-to-noise ratio (SNR) at the LU. To achieve this, one of the selection mechanisms of [10] was proposed, wherein one transmitter having the best instantaneous SNR at the LU is selected first for data transmissions, and then one additional transmitter causing the least interference at the LU is selected as a jamming transmitter.

If we apply joint data and jamming transmissions in PLS

K. J. Kim and P. V. Orlik are with Mitsubishi Electric Research Laboratories (MERL), Cambridge, MA 02139 USA (e-mail: kkim@merl.com; porlik@merl.com)

H. Liu is with Shandong Jiaotong University, Jinan, China (e-mail: liuhongwu@sdjtu.edu.cn)

M. Wen is with South China University of Technology, Guangzhou, China (email: eemwwen@scut.edu.cn)

H. V. Poor is with the Department of Electrical Engineering, Princeton University, Princeton, NJ 08544 USA (e-mail: poor@princeton.edu).

Parts of this paper were presented at the 2019 IEEE Global Communications Conference [1].

[1]In addition to [20], dCDD was proposed for the spectrum sharing system [21].

systems, a jamming transmission interferes with the LU [9], [10], [14], [17] intrinsically, so that it should be considered in receiver processing. In contrast to these works, the dCDD scheme can avoid interference at the LU, even for multiple simultaneous jamming transmissions [12] when the considered transmitters are supported by dCDD. Thus, the LU can remove this interference.

Most of the existing works assume CSI [2], [9], [10], [13], partial CSI [12], [23], or statistical CSI [11], [14], [15], [17] at the transmitting side by the explicit feedback. However, as a practical setting, this paper assumes that the EU is in a passive mode, so that neither perfect CSI of the legitimate channels (LU channels) nor that of the eavesdropper channels (EU channels) is available by the LU via an explicit feedback [3], [16]. Note that transmit antenna selection (TAS) was proposed by [3] for secrecy enhancement. However, TAS is mainly applied for the selection of antennas installed at the same transmitter, so that [3] does not provide a method for joint data and jamming transmissions. In [16], cooperative AN transmission was proposed under an individual power constraint for each node. Although a joint selection scheme for the data and interfering transmitters was proposed by [12], it is inappropriate for this new practical setting which does not allow explicit CSI feedback of the EU channel. An AN assisted secure transmission for a distributed antenna system (DAS) was proposed in [23] using large-scale CSI available at the transmitter. Although, the employed dCDD can be recognized as the DAS [21], this paper does not assume this type of CSI at the transmitter since explicit feedback is not allowed from the LU.

A. Problems

- Tight time synchronization among remote radio heads (RRHs): Since RRHs are connected to the central control unit (CU) via wireless backhaul and implemented by only simple hardware, a tight synchronization among them is not achievable. For this reason, synchronous signal reception may not be achievable at the LU, which influences the objective of dCDD, namely removing ISI caused by frequency selective fading channel and multiple transmissions. Thus, it is required to develop another distributed transmit diversity scheme, called distributed asynchronous cyclic delay diversity (dACDD), that supports asynchronous signal reception at the LU. A similar transmit diversity scheme was proposed for asynchronous cooperative relay network [24]. However, the author of [24] employed the space-time transmission.
- Selection scheme of the data RRH and interfering RRHs: To degrade the reception quality at the EU, it is preferable to use as many transmitters as possible as interfering transmitters without causing interference at the LU. Thus, we need to develop a practical solution to overcome the limitation of the existing works which support only one jamming transmitter [9]–[11], [16], [17].

B. Contributions

To the best of our knowledge, the dACDD scheme has not previously been developed and applied to distributed CP-SC systems with the objective of minimizing information leakage to a passive EU without explicit feedback of CSI. Thus, the main contributions made by the present paper include the following:

C_1 : We introduce a new operation at each RRH to support dACDD at the LU even for asynchronous CP-SC reception due to different arrival times of the signals transmitted over the legitimate channels. It is verified that a simple additional operation to assign cyclic delay diversity (CDD) delay is necessary depending on the relative arrival time difference at the LU.

C_2 : We introduce a new selection scheme for the data RRH and interfering RRHs under the framework of dACDD in the presence of one passive EU. Without requiring explicit feedback of perfect CSI by the LU, only limited information of the channels is required by an implicit feedback. From a standpoint that does not require perfect CSI, the proposed selection scheme is somewhat similar to the solution introduced by [7], [10]–[12], [17], [23], and [25]. However, the proposed scheme has the following differences from them.

- C_{21}: In contrast to [12] and [23], the proposed selection scheme does not require perfect CSI of the EU channels [12] and statistical CSI of the large-scale fading [23].
- C_{22}: A greater instantaneous SNR than that of the simpler random selection scheme proposed in [7] and [25] can be achieved at the LU with the use of dACDD.
- C_{23}: Since the proposed selection scheme assigns more RRHs to transmit artificial interfering sequences (AISs) to the EU, it makes the SINR at the EU much more reduced comparing with the schemes proposed by [10], [11], and [17].

C_3 : We verify the diversity order on the secrecy outage probability (SOP) based on the asymptotic analysis. We prove that the channel parameters of the small-scale legitimate channels and the number of RRHs supported by dACDD determine the diversity gain. The large-scale fading has no effect on the diversity gain. Moreover, we verify that this achievable diversity gain is the same, irrespective of which RRH acts as the data RRH in the independent but not identically distributed (i.n.i.d.) frequency selective fading channels.

The rest of the paper is organized as follows. In Section II, the system and channel models are introduced. The method for selecting the data and interfering RRHs based on dCDD is also described. In Section III, the receive SNR and SINR at the LU and EU are respectively computed. Furthermore, the conditional and marginal SOPs and probability of non-zero achievable secrecy rates are respectively studied. Simulation results are illustrated in Section IV and conclusions are drawn in Section V.

Notation: The superscript $(\cdot)^H$ denotes complex conjugate transposition; $E\{\cdot\}$ denotes expectation; $\boldsymbol{I}_N$ denotes an $N \times N$ identity matrix; $\mathbf{0}$ denotes an all-zero matrix of with an appropriate size; $\|\boldsymbol{a}_n\|$ denotes the Euclidean norm of a vector

$\boldsymbol{a}_n$; $\mathcal{CN}\left(\mu, \sigma^2\right)$ denotes a complex Gaussian distribution with mean μ and variance σ^2; $\mathbb{N}_0$ denotes the set of non-negative integers; $\mathbb{C}^{m\times n}$ denotes the vector space of all $m \times n$ complex matrices; and $F_\varphi(\cdot)$ denotes the cumulative distribution function (CDF) of the random variable (RV) φ, whereas its PDF is denoted by $f_\varphi(\cdot)$. The binomial coefficient is denoted by $\binom{n}{k} \triangleq \frac{n!}{(n-k)!k!}$. The lth element of a vector $\boldsymbol{a}$ is denoted by $\boldsymbol{a}(l)$; and $\mathfrak{N}(\boldsymbol{a})$ denotes the cardinality of a vector $\boldsymbol{a}$. When the dth element of a vector $\boldsymbol{a}_b$ is excluded, then it is denoted by $\boldsymbol{a}_{b\setminus d}$. For a set of continuous random variables, $\{x_1, x_2, \ldots, x_N\}$, $x_{\langle i\rangle}$ denotes the ith smallest random variable, so that it becomes the ith order statistic.

II. System and Channel Models

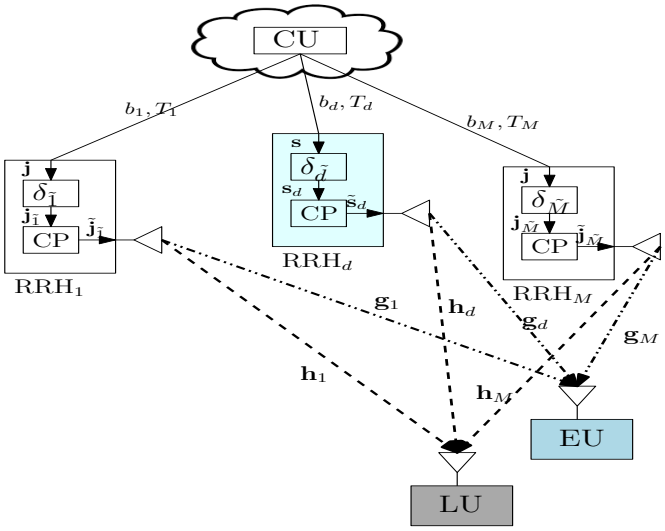

Fig. 1. Illustration of the considered cooperative system, which communicates with the CU via wireless backhaul links $\{b_1, \ldots, b_M\}$. Based on the dACDD scheme, M RRHs communicate with the LU through legitimate channels $\{\boldsymbol{h}_m,\ \forall m\}$. Wireless communications made by RRHs and LU can be intercepted by an EU through eavesdropper channels $\{\boldsymbol{g}_m, \forall m\}$. One RRH highlighted in a different color is assigned as the data RRH, whereas the remaining $(M-1)$ RRHs are assigned as the interfering RRHs.

An illustration of the considered distributed CP-SC system is provided in Fig. 1. A plurality of RRHs are deployed over a geographical area. Wireless backhaul links, $\{b_m, \forall m\}$, are configured to provide broadband wireless access to M RRHs via the CU. Every node in the system is assumed to be equipped with a single antenna, due to practical constraints on the hardware complexity and power limitation, which is a realistic setting for the RRH deployment. With the aid of the CU, cooperative communications occur between the RRHs and LU in the presence of an EU. To increase PLS of the distributed CP-SC system, one of the RRHs is assigned as the data RRH, while the remaining RRHs are assigned as interfering RRHs that transmit AISs. As the AIS, the Zadoff-Chu sequence (ZCS) [12], [26], [27] is considered since its amplitude is constant in the time (frequency) domain and its autocorrelation is zero for all non-zero cyclic shifts [27]. The seed of the ZCS is shared only among the legitimate CU, RRHs, and LU. Each RRH acts either as the data RRH or as the interfering RRH by the control of the CU. To assure an interference free reception at the LU, the dACDD scheme is employed between the RRHs and LU under the control of the CU. In the considered system, the EU is assumed to be in a passive mode, so that perfect CSI of the EU channels is unknown at the CU, RRHs, and LU. This is one of the key differences in the system settings compared with those of [12]. Due to this restriction, optimal selections proposed by [9], [10], [28]–[31], are not available for the selection of interfering RRHs. Especially, [28]–[31] proposed to use maximum ratio transmission (MRT) scheme.

A. Channel model

A small-scale frequency selective fading channel from the mth RRH to the LU is assumed, and denoted by $\boldsymbol{h}_m$ with $\mathfrak{N}(\boldsymbol{h}_m) = N_{h,m}$, whose elements are assumed to be independent and identically distributed according to $\mathcal{CN}(0,1)$ [12], [32], [33]. The distance-dependent large scale fading over the channel $\boldsymbol{h}_m$ is denoted by $\alpha_{h,m}$. For a distance $d_{1,m}$ from the mth RRH to the LU, $\alpha_{h,m}$ is given by $\alpha_{h,m} = (d_{1,m})^{-\epsilon}$, where ϵ denotes the path loss exponent. The LU is placed at a specific location with respect to the RRHs, and, thus, i.n.i.d. frequency selective fading channels from the RRHs to the LU are also assumed. The LU is assumed to have knowledge of the number of multipath components of the LU channels, by either sending the training sequence [34] or adding the pilot as the suffix to each symbol block [35], [36]. Similarly, a small-scale frequency selective fading channel from the mth RRH to the EU is considered and denoted by $\boldsymbol{g}_m$ with $\mathfrak{N}(\boldsymbol{g}_m) = N_{g,m}$, whose elements are assumed to be independent and identically distributed according to $\mathcal{CN}(0,1)$. The distance-dependent large scale fading over the channel $\boldsymbol{g}_m$ is denoted by $\alpha_{g,m}$. For a distance $d_{2,m}$ from the mth RRH to the EU, $\alpha_{g,m}$ is given by $\alpha_{g,m} = (d_{2,m})^{-\epsilon}$.

B. Summary of dCDD

To convert the multiple-input single-output channel into an ISI-free single-input single-output channel, the first condition is to remove the ISI caused from the frequency selective fading channel by adding the last N_{CP} symbols, to the front of the block symbol, $\boldsymbol{s} \in \mathbb{C}^{Q\times 1}$, comprising Q modulated symbols. The cyclic-prefix (CP) length, N_{CP} is determined by $N_{\mathrm{CP}} \geq \max\{N_{h,1}, \ldots, N_{h,M}\}$. From CP-SC transmissions, N_{CP} and Q jointly determine the maximum allowable number of RRHs for dCDD operation, which is given by $K = \left\lfloor \frac{Q}{N_{\mathrm{CP}}} \right\rfloor$, where $\lfloor\cdot\rfloor$ denotes the floor function. Without loss of generality, we consider only an underpopulated system, so that we have $M \leq K$.

In addition, the LU makes a very accurate channel estimation, and then specifies RRH's order by the magnitudes of available channel estimates in an ascending order as $\alpha_{h,\langle 1\rangle}\|\boldsymbol{h}_{\langle 1\rangle}\|^2 \leq \alpha_{h,\langle 2\rangle}\|\boldsymbol{h}_{\langle 2\rangle}\|^2 \leq \ldots \leq \alpha_{h,\langle M\rangle}\|\boldsymbol{h}_{\langle M\rangle}\|^2$. Based on this determined order, the LU feeds back only $\langle M\rangle \in \mathbb{N}_0$, which specifies the index of the strongest legitimate channel. Since the CU has knowledge of M, independent of the EU channels, the CU generates a random vector

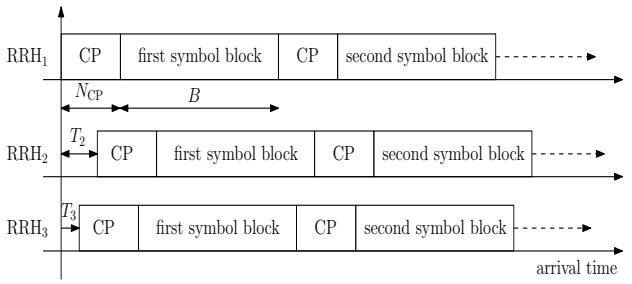

Fig. 2. One example of an asynchronous reception at the LU with relative arrival time differences $T_2 \in \mathbb{N}_0$ and $T_3 \in \mathbb{N}_0$.

$\mathbb{S}_M \in \mathbb{N}_0^M$, which is composed of the randomly permuted integers from 1 to M. Since a random permutation does not change the performance of the CP-SC system with dCDD [20], $\mathbb{S}_M$ can be anyone from a group of $M!$ random vectors. From PLS perspective, the CU shares $\mathbb{S}_M$ only with the RRHs and LU.

Without loss of generality, we assume that RRH_1's signal arrives at the LU first. Due to different propagation delays from RRHs to the LU, a relative time difference between the arrival time of the signal transmitted from RRH_m and that of the signal transmitted from RRH_1 is denoted by $T_m \in \mathbb{N}_0$. One example of asynchronous signal reception at the LU is illustrated in Fig. 2. This paper assumes that the relative arrival time differences are all less than N_{CP}, so that $T_2 < N_{\mathrm{CP}}$ and $T_3 < N_{\mathrm{CP}}$ [24]. Even for the asynchronous signal reception at the LU, the CU needs to assign a unique CDD delay to the mth RRH to remove ISI caused by multiple CP-SC transmissions as follows:

$$\Delta_m = (\mathbb{S}_M(m) - 1)N_{\mathrm{CP}}. \tag{1}$$

However, in general, $T_m \neq \Delta_m$ and $T_m < \Delta_m$. Based on T_m and Δ_m, the CU forces RRH_m to apply CDD delay by an amount of $\delta_m \triangleq \Delta_m - T_m$. Thus, an extensive scheme of dCDD, called dACDD, is developed, in which the CDD delay is determined by the relative arrival time differences. In contrast to dCDD, which is working only for the tightly synchronized RRHs [12], dACDD can be working even for the un-synchronized RRHs. Since the CDD delay is determined by a random arrival time difference for the signals transmitted over the legitimate channels and the randomized vector $\mathbb{S}_M$, independent of the EU channels, dACDD can improve PLS in a different way from [12]. However, since dACDD requires knowledge of $\{T_m\}_{m=1}^M$ at the CU, an additional feedback is required by the LU.

C. dACDD operation based on the proposed selection of data and interfering RRHs

Upon utilizing M and $d \triangleq \langle M \rangle$, which are available at the CU, the CU is able to choose RRH_d, as the data RRH that transmits the data symbols to the LU, and then assigns remaining $(M-1)$ RRHs as the interfering RRHs that transmit the AISs simultaneously to the LU and EU. According to Fig.1, the symbol block is formed as $\tilde{\boldsymbol{s}}_d \triangleq \begin{bmatrix} \boldsymbol{s}_d(Q - N_{\mathrm{CP}} + 1 : Q, 1) \\ \boldsymbol{s}_d \end{bmatrix} \in \mathbb{C}^{(Q+N_{\mathrm{CP}})\times 1}$, where $\boldsymbol{s}_d$ is obtained from $\boldsymbol{s}$ by applying the corresponding CDD delay as follows: $\boldsymbol{s}_d = \boldsymbol{P}_{Q,\delta_d}\boldsymbol{s}$, with $\delta_d \triangleq \Delta_d - T_d$, and then transmitted via $\boldsymbol{h}_d$. In contrast, when $(M-1)$ RRHs, denoted by $\{\mathrm{RRH}_m\}_{m=1,m\neq d}^M$, are assigned as the interfering RRHs, one of the resulting AISs is generated as $\boldsymbol{j}_m = \boldsymbol{P}_{Q,\delta_m}\boldsymbol{j}$, where $\boldsymbol{j}$ is the original AIS. For $\boldsymbol{j}_m$, a CP of N_{CP} symbols is appended to the front of $\boldsymbol{j}_m$; that is, we can have $\tilde{\boldsymbol{j}}_m \triangleq \begin{bmatrix} \boldsymbol{j}_m(Q - N_{\mathrm{CP}} + 1 : Q, 1) \\ \boldsymbol{j}_m \end{bmatrix} \in \mathbb{C}^{(Q+N_{\mathrm{CP}})\times 1}$. After that $\tilde{\boldsymbol{j}}_m$ is transmitted sequentially to the LU via $\boldsymbol{h}_m$. The EU receives $\tilde{\boldsymbol{j}}_m$ via $\boldsymbol{g}_m$. In the representation of $\boldsymbol{s}_d$ and $\{\boldsymbol{j}_m\}_{m=1,m\neq d}^M$, $\boldsymbol{P}_{Q,\delta_d}$ and $\{\boldsymbol{P}_{Q,\delta_m}\}_{m=1,m\neq d}^M$ respectively denote the permutation matrices obtained by circularly shifting down $\boldsymbol{I}_Q$ by δ_d and $\{\delta_m\}_{m=1,m\neq d}^M$.

D. Received signals at the LU and EU

After the removal of the CP signal, the received signal at the LU is given by

$$\boldsymbol{r}_L = \sqrt{P_T\alpha_{h,d}}\boldsymbol{\Pi}_d\boldsymbol{H}_d\boldsymbol{P}_{Q,\delta_d}\boldsymbol{s} + \sum_{m=1,m\neq d}^{M} \sqrt{P_J\alpha_{h,m}}\boldsymbol{\Pi}_m\boldsymbol{H}_m\underbrace{\boldsymbol{P}_{Q,\delta_m}\boldsymbol{j}}_{\boldsymbol{j}_m} + \boldsymbol{z}_L \tag{2}$$

where $\boldsymbol{\Pi}_m$ denotes the $Q \times Q$ orthogonal permutation matrix obtained by circularly shifting down $\boldsymbol{I}_Q$ by T_m rows, and P_J is the transmission power for AIS transmissions. The additive vector noise over the LU channels is denoted by $\boldsymbol{z}_L \sim \mathcal{CN}(\boldsymbol{0}, \sigma_z^2\boldsymbol{I}_Q)$. From the properties of the ZCS, we have $E\{\boldsymbol{j}\} = \boldsymbol{0}$, and $E\{\boldsymbol{j}\boldsymbol{j}^H\} = \boldsymbol{I}_Q$. Furthermore, since $\boldsymbol{P}_{Q,\delta_m}$ is an unitary matrix, we have $E\{\boldsymbol{j}_m\} = \boldsymbol{0}$, and $E\{\boldsymbol{j}_m(\boldsymbol{j}_m)^H\} = \boldsymbol{I}_Q$. We can summarize several benefits of dACDD from PLS perspective as follows:

1) A set of different relative arrival time differences $\{T_m\}_{m=2}^M$ is independent of that of asynchronous or synchronous reception from the RRHs to the EU, so that $\{T_m\}_{m=2}^M$ can be recognized as a set of random variables to the EU. Furthermore, the randomized vector $\mathbb{S}_M$ is not available at the EU. Thus, a set of AISs, $\{\boldsymbol{j}_m\}_{m=1,m\neq d}^M$, obtained from the ZCS by applying the CDD delays determined by $\{T_m\}_{m=1,m\neq d}^M$ and $\mathbb{S}_M$, is known only to the RRHs and LU. In addition, the seed of the ZCS is shared only among the legitimate CU, RRHs, and LU. These additional features utilized by dACDD increase uncertainty in decoding AISs by the EU, so that PLS can be improved.

Utilizing ISI-free reception at the LU, we can rewrite (2) as follows:

$$\boldsymbol{r}_L = \sqrt{P_T\alpha_{h,d}}\boldsymbol{\Pi}_d\boldsymbol{H}_d\boldsymbol{P}_{Q,\delta_d}\boldsymbol{s} + \boldsymbol{z}_L. \tag{3}$$

Note that with reliable channel estimate and a known seed of the ZCS at the LU, we can obtain (3). In contrast, the received signal at the EU is given by

$$\boldsymbol{r}_E = \sqrt{P_T\alpha_{g,d}}\breve{\boldsymbol{\Pi}}_d\boldsymbol{G}_d\boldsymbol{P}_{Q,\delta_d}\boldsymbol{s} + \sum_{m=1,m\neq d}^{M} \sqrt{P_J\alpha_{g,m}}\breve{\boldsymbol{\Pi}}_m\boldsymbol{G}_m\underbrace{\boldsymbol{P}_{Q,\delta_m}\boldsymbol{j}}_{\boldsymbol{j}_m} + \boldsymbol{z}_E \tag{4}$$

where $\boldsymbol{G}_d$ and $\boldsymbol{G}_m$ are right circulant matrices specified by the equivalent channel vectors $\boldsymbol{g}_d$ and $\boldsymbol{g}_m$, respectively. Note that $\alpha_{g,m}$ is used to model the distance-dependent large scale fading from the mth RRH to EU. A set of relative arrival difference from RRHs to EU, $\{\breve{T}_m\}_{m=1}^M$ specifies $\breve{\boldsymbol{\Pi}}_m$. We also assume that $\boldsymbol{z}_E \sim \mathcal{CN}(\boldsymbol{0}, \sigma_z^2 \boldsymbol{I}_Q)$. Note that a relative arrival time difference T_m is independent of the channels from RRHs to EU, that is, $T_m \neq \breve{T}_m$. Most importantly, $\mathbb{S}_M$ is shared only by the legitimate CU, RRHs, and LU.

Due to CP-SC transmissions and the use of unitary permutation matrices, $\{\boldsymbol{\Pi}_m\}_{m=1}^M$, $\{\boldsymbol{H}_m\}_{m=1}^M$, $\{\boldsymbol{P}_{Q,\delta_m}\}_{m=1}^M$, $\{\breve{\boldsymbol{\Pi}}_m\}_{m=1}^M$, and $\{\boldsymbol{G}_m\}_{m=1}^M$ are right circulant matrices. The product of two right circulant matrices is again right circulant and commutative, so that we can alternatively express (3) as follows:

$$\boldsymbol{r}_L = \sqrt{P_T \alpha_{h,d}} \boldsymbol{H}_d \boldsymbol{\Pi}_d \boldsymbol{P}_{Q,\delta_d} \boldsymbol{s} + \boldsymbol{z}_L \tag{5}$$

where the product of two permutation matrices, $\boldsymbol{\Pi}_d \boldsymbol{P}_{Q,\delta_d}$, circulates $\boldsymbol{s}$ by an amount of Δ_d. However, from (4), $\breve{\boldsymbol{\Pi}}_m \boldsymbol{P}_{Q,\delta_m}$ can exactly circulate $\boldsymbol{j}$ by an amount of Δ_m only when δ_m is exactly known at the EU.

III. Performance Analysis

To study the performance of the proposed PLS system comprising the data and interfering RRHs under the framework of dACDD, we need to know the distributions of the receive SNR and SINR at the LU and EU, respectively.

A. Receive SNR at the LU over i.n.i.d. frequency selective fading channel

In the sequel, the mth receive SNR at the LU, achievable by the mth legitimate channel, is denoted by $\gamma_{L,m} \triangleq \frac{P_T \alpha_{h,m}}{\sigma_z^2} \|\boldsymbol{h}_m\|^2 \triangleq \tilde{\alpha}_{h,m} \|\boldsymbol{h}_m\|^2$, where $\tilde{\alpha}_{h,m} \triangleq \frac{P_T \alpha_{h,m}}{\sigma_z^2}$. Note that in this definition, we use the fact that $\boldsymbol{\Pi}_m \boldsymbol{H}_m \boldsymbol{P}_{Q,\delta_m}$ is a right circulant matrix.

For i.n.i.d. frequency selective fading channels, the probability that the RRH_d is chosen as the data RRH, is distributed non-uniformly due to a different distance from a particular RRH to the LU, and a non-identical frequency selective fading channel. Since CSI of the eavesdropper channels is not available and $\mathbb{S}_M$ is used at the CU, the legitimate channels are mainly used in the computation of $P_r(d) \triangleq P_r(\mathrm{RRH}_d \text{ is working as data RRH})$ in the following theorem.

Theorem 1: For i.n.i.d. frequency selective LU channels, $P_r(d)$ is given by

$$P_r(d) = 1 + \frac{1}{\Gamma(N_{h,d})(\tilde{\alpha}_{h,d})^{N_{h,d}}} \sum_{m=1}^{M-1} (-1)^m \Upsilon_d \Gamma(N_{h,d} + \tilde{l}_d) \prod_{t=1}^{m} \Big(\frac{(\tilde{\boldsymbol{\beta}}_{h\setminus d}(q_t))^{\ell_t}}{\ell_t!} \Big) \big(\tilde{\beta}_d + \frac{1}{\tilde{\alpha}_{h,d}} \big)^{-(N_{h,d} + \tilde{l}_d)} \tag{6}$$

where $\tilde{\beta}_d \triangleq \sum_{t=1}^{m} \frac{1}{\tilde{\boldsymbol{\beta}}_{h\setminus d}(q_t)}$, $\tilde{l}_d \triangleq \sum_{t=1}^{m} \ell_t$, $\Upsilon_d \triangleq \sum_{q_1=1}^{M-m} \cdots \sum_{q_m=q_{m-1}+1}^{M-1} \sum_{\ell_1=0}^{N_{h,q_1}-1} \cdots \sum_{\ell_m=0}^{N_{h,q_m}-1}$, and $\tilde{\boldsymbol{\beta}}_{h\setminus d} \triangleq [\tilde{\alpha}_{h,1}, \ldots, \tilde{\alpha}_{h,d-1}, \tilde{\alpha}_{h,d+1}, \ldots, \tilde{\alpha}_{h,M}]^T$. Recall that $\tilde{\boldsymbol{\beta}}_{h\setminus d}(q_t)$ denotes the q_tth element of $\tilde{\boldsymbol{\beta}}_{h\setminus d}$.

Proof: See Appendix A. ∎

Note that a set of multipath components and $\tilde{\boldsymbol{\beta}}_{h\setminus d}$ jointly contribute to $P_r(d)$. Thus, when the channels are distributed according to the i.i.d. frequency selective fading with the same number of multipath components, then we can have $P_r(d) = \frac{1}{M}, \forall d$.

According to (3), the conditional receive SNR at the LU on the channel $\boldsymbol{h}_d$, which is chosen for data transmissions, is given by

$$\gamma_{L,d} = \tilde{\alpha}_{h,d} \sum_{l=1}^{N_{h,d}} |\boldsymbol{h}_d(l)|^2. \tag{7}$$

Now the CDF of $\gamma_{L,d}$ is given by

$$\begin{aligned} F_{\gamma_{L,d}}(x) &= P_r\big(\gamma_{L,d} < x | d = \underset{j\in[1,\ldots,M]}{\operatorname{argmax}} (\gamma_{L,j})\big) \\ &= \frac{P_r\big(\gamma_{L,d} < x, d = \operatorname{argmax}_{j\in[1,\ldots,M]}(\gamma_{L,j})\big)}{P_r\big(d = \operatorname{argmax}_{j\in[1,\ldots,M]}(\gamma_{L,j})\big)} \\ &= \frac{1}{P_r(d)} \underbrace{\int_0^x f_{\gamma_{L,d}}(t) \prod_{j=1, j\neq d}^{M} F_{\gamma_{L,j}}(t) dt}_{J_1} \end{aligned} \tag{8}$$

where $F_{\gamma_{L,j}}(x) = 1 - e^{-\frac{x}{\tilde{\alpha}_{h,j}}} \sum_{l=0}^{N_{h,j}-1} \frac{1}{l!} \Big(\frac{x}{\tilde{\alpha}_{h,j}} \Big)^l$. Applying the same procedure provided in Appendix A, J_1 can be evaluated as (9), provided at the top of the next page. In (9), $\mathbb{X}_{L_1} \triangleq \sum_{l_1=0}^{N_{h,d}-1} \frac{1}{\Gamma(l_1+1)}$, and $\gamma_l(\cdot,\cdot)$ denotes the lower incomplete gamma function [37, Eq. (8.350.1)]. One additional term, $\mathbb{X}_{L_2}$, is defined in Appendix B.

Proposition 1: When the dth RRH is selected as the data RRH, it provides the LU with the conditional receive SNR, $\gamma_{L,d}$, over the i.n.i.d frequency selective legitimate channels, which is distributed as (10), provided at the top of the next page.

Proof: According to (9), we can readily derive (10). ∎

B. Receive SINR at the EU over i.n.i.d. frequency selective fading channels

From (4), the received signal at the EU consists of the desired signal being intercepted, non-decodable interference by the AISs, and noise. Thus, the receive signal power, $S_{E,d}$, and noise-plus-interference power due to interfering signal, $N_{E,d}$, at the EU are respectively given by

$$\begin{aligned} S_{E,d} &= P_T \alpha_{g,d} \sum_{l=1}^{N_{g,d}} |\boldsymbol{g}_d(l)|^2 \text{ and} \\ N_{E,d} &= P_J \sum_{m=1, m\neq d}^{M} \alpha_{g,m} \sum_{l=1}^{N_{g,m}} |\boldsymbol{g}_m(l)|^2 + \sigma_z^2 \end{aligned} \tag{11}$$

where $S_{E,d}$ is the signal power provided by the dth data RRH. Note that $\breve{\boldsymbol{\Pi}}_m \boldsymbol{G}_m \boldsymbol{P}_{Q,\delta_m}$ is also right circulant. One of the legitimate channels, the one that provides the greatest channel gain, is selected for the dada RRH under the control of the

$$J_1 = F_{\gamma_{L,d}}(x) + \frac{1}{\Gamma(N_{h,d})(\tilde{\alpha}_{h,d})^{N_{h,d}}} \sum_{m_1=1}^{M-1} (-1)^{m_1} \Upsilon_d \prod_{t=1}^{m_1} \Big(\frac{1}{\ell_t! (\tilde{\boldsymbol{\beta}}_{h\setminus d}(q_t))^{\ell_t}} \Big)$$
$$\gamma_l \big(N_{h,d} + \tilde{l}_d, \big(\tilde{\beta}_d + \frac{1}{\tilde{\alpha}_{h,d}}\big)x \big) \big(\tilde{\beta}_d + \frac{1}{\tilde{\alpha}_{h,d}}\big)^{-(N_{h,d}+\tilde{l}_d)}$$
$$= 1 - \mathbb{X}_{L_1} e^{-\frac{x}{\tilde{\alpha}_{h,d}}} x^{l_1} + \mathbb{X}_{L_2} \Big(1 - \sum_{m_2=0}^{N_{h,d}+\tilde{l}_d-1} \frac{1}{\Gamma(m_2+1)} \big(\tilde{\beta}_d + \frac{1}{\tilde{\alpha}_{h,d}}\big)^{m_2} x^{m_2} e^{-(\tilde{\beta}_d + \frac{1}{\tilde{\alpha}_{h,d}})x} \Big). \quad (9)$$

$$F_{\gamma_{L,d}}(x) = \frac{1}{P_r(d)} - \frac{\mathbb{X}_{L_1}}{P_r(d)} e^{-\frac{x}{\tilde{\alpha}_{h,d}}} x^{l_1} + \frac{\mathbb{X}_{L_2}}{P_r(d)} \Big(1 - \sum_{m_2=0}^{N_{h,d}+\tilde{l}_d-1} \frac{1}{\Gamma(m_2+1)} \big(\tilde{\beta}_d + \frac{1}{\tilde{\alpha}_{h,d}}\big)^{m_2} x^{m_2} e^{-(\tilde{\beta}_d + \frac{1}{\tilde{\alpha}_{h,d}})x} \Big). \quad (10)$$

CU. In addition, the remaining $(M-1)$ RRHs are assigned as the set of interfering RRHs. Thus, $S_{E,d}/N_{E,d}$ decreases in general as the number of RRHs increases, which is beneficial for increasing the security of the proposed cooperative system. Note that the eavesdropper channels are independent of the legitimate channels, so that the conditional SINR at the EU is given by

$$\gamma_{E,d} \triangleq \frac{S_{E,d}}{N_{E,d}} = \frac{\tilde{\alpha}_{g,d} \sum_{l=1}^{N_{g,d}} |\boldsymbol{g}_d(l)|^2}{\sum_{m=1,m\neq d}^{M} \tilde{\alpha}_{g,m} \sum_{l=1}^{N_{g,m}} |\boldsymbol{g}_m(l)|^2 + 1} \triangleq \frac{A}{B+1} \quad (12)$$

where $\tilde{\alpha}_{g,d} \triangleq \frac{P_T \alpha_{g,d}}{\sigma_z^2}$ and $\tilde{\alpha}_{g,m} \triangleq \frac{P_J \alpha_{g,m}}{\sigma_z^2}$. In addition, $A \triangleq \tilde{\alpha}_{g,d} \sum_{l=1}^{N_{g,d}} |\boldsymbol{g}_d(l)|^2$ and $B \triangleq \sum_{m=1,m\neq d}^{M} \tilde{\alpha}_{g,m} \sum_{l=1}^{N_{g,m}} |\boldsymbol{g}_m(l)|^2$. Note that $\tilde{\alpha}_{g,d}$ is multiplied by P_T, whereas $\{\tilde{\alpha}_{g,m}\}_{m=1,m\neq d}^{M}$ are multiplied by P_J. The corresponding PDF of $\gamma_{E,d}$ is derived in the following theorem.

Theorem 2: For i.n.i.d. frequency selective eavesdropper channels, the distribution of the receive SINR at the EU is given by (13), provided at the top of the next page. In (13), the jth element of $\boldsymbol{\theta}_{m_3\setminus d}$ is defined in Appendix C. In addition, $\tilde{\boldsymbol{\beta}}_{g\setminus d}(m_3)$ denotes the m_3th element of $\tilde{\boldsymbol{\beta}}_{g\setminus d}$, which is defined by $\tilde{\boldsymbol{\beta}}_{g\setminus d} \triangleq [\tilde{\alpha}_{g,1}, \ldots, \tilde{\alpha}_{g,d-1}, \tilde{\alpha}_{g,d+1}, \ldots, \tilde{\alpha}_{g,M}]^T$, and $\mathbb{X}_E$ is defined in Appendix B.

Proof: See Appendix C. ∎

C. Secrecy outage probability

The conditional transmission capacity achieved by the dth legitimate transmissions is given by

$$C_{R,d} = \log_2(1 + \gamma_{L,d}) \quad (14)$$

whereas the corresponding interceptable capacity is defined as [3]:

$$C_{E,d} = \log_2(1 + \gamma_{E,d}). \quad (15)$$

Based on Eqs. (14) and (15), the conditional secrecy capacity $C_{s,d}$ is defined as follows:

$$C_{S,d} = [C_{R,d} - C_{E,d}]^+ \quad (16)$$

where $[x]^+ \triangleq \max(x, 0)$.

At a given secrecy rate R_s, the conditional secrecy outage probability (SOP) is defined by

$$P_{d,\text{out}}(R_s) = P_r(C_{s,d} < R_s)$$
$$= \int_0^\infty F_{\gamma_{L,d}}(J_R(1+x) - 1) f_{\gamma_{E,d}}(x) dx \quad (17)$$

where $J_R \triangleq 2^{R_s}$.

According to (17), the closed form expression for $P_{d,\text{out}}(R_s)$, can be derived in the next theorem.

Theorem 3: For i.n.i.d. frequency selective fading over the entire legitimate and eavesdropper channels, the proposed CP-SC system improves PLS by employing dACDD, which supports simultaneous data and interference transmissions. The achievable conditional SOP at secrecy rate R_s is given by (18), provided at the top of the next page. In (18), we have defined $\Delta J_R \triangleq J_R(\tilde{\beta}_d + \frac{1}{\tilde{\alpha}_{h,d}}) + \frac{1}{\tilde{\alpha}_{g,d}}$, and $G_{p,q}^{m,n}\Big(t \Big| \begin{matrix} a_1, \ldots, a_n, a_{n+1}, \ldots, a_p \\ b_1, \ldots, b_m, b_{m+1}, \ldots, b_q \end{matrix}\Big)$ denotes the Meijer G-function [37, Eq. (9.301)]. In addition, $\mathbb{X}_{P_1}$ and $\mathbb{X}_{P_2}$ are defined in Appendix B.

Proof: See Appendix D. ∎

Proposition 2: Based on (18), the marginal SOP achieved by the proposed dACDD based PLS system is given by

$$P_{\text{out}}(R_s) = \sum_{d=1}^{M} P_{d,\text{out}}(R_s) P_r(d). \quad (19)$$

Proof: At each of the CP-SC transmissions, only one RRH is selected as the data RRH, so that the selection of the data RRH is mutually exclusive and independent of each other. Thus, we can have (19). ∎

D. Probability of non-zero achievable secrecy rate

In the following, we will derive the probability of non-zero achievable secrecy rate when the dth RRH is known to be the data RRH.

$$f_{\gamma_{E,d}}(x)=\frac{1}{\Gamma(N_{g,d})(\tilde{\alpha}_{g,d})^{N_{g,d}}}\sum_{m_3=1,m_3\neq d}^{M}\sum_{j=1}^{N_{g,m_3}}\sum_{l_2=0}^{N_{g,d}}\frac{(-1)^{m_3}\boldsymbol{\theta}_{m_3\backslash d}(j)}{\Gamma(j)}\binom{N_{g,d}}{l_2}\Gamma(l_2+j)$$
$$e^{-\frac{x}{\tilde{\alpha}_{g,d}}}(x)^{N_{g,d}-1}\big(\frac{x}{\tilde{\alpha}_{g,d}}+\frac{1}{\tilde{\boldsymbol{\beta}}_{g\backslash d}(m_3)}\big)^{-(l_2+j)}$$
$$=\mathbb{X}_E e^{-\frac{x}{\tilde{\alpha}_{g,d}}}(x)^{N_{g,d}-1}\big(\frac{x}{\tilde{\alpha}_{g,d}}+\frac{1}{\tilde{\boldsymbol{\beta}}_{g\backslash d}(m_3)}\big)^{-(l_2+j)}. \quad (13)$$

$$P_{d,\text{out}}(R_s)=\frac{1}{P_r(d)}-\frac{\mathbb{X}_{P_1}}{P_r(d)}G_{2,1}^{1,2}\Big(\frac{\tilde{\boldsymbol{\beta}}_{g\backslash d}(m_3)}{\tilde{\alpha}_{g,d}}\big(\frac{J_R}{\tilde{\alpha}_{h,d}}+\frac{1}{\tilde{\alpha}_{g,d}}\big)^{-1}\Big|\begin{matrix}1-j_2-N_{g,d},1-l_2-j\\0\end{matrix}\Big)+$$
$$\frac{\mathbb{X}_{L_2}}{P_r(d)}\Big[1-\mathbb{X}_{P_2}G_{2,1}^{1,2}\Big(\frac{\tilde{\boldsymbol{\beta}}_{g\backslash d}(m_3)}{\tilde{\alpha}_{g,d}}\big(\Delta J_R\big)^{-1}\Big|\begin{matrix}1-j_3-N_{g,d},1-l_2-j\\0\end{matrix}\Big)\Big]. \quad (18)$$

Theorem 4: For i.n.i.d. frequency selective fading over the entire legitimate and eavesdropper channels, the proposed CP-SC based secrecy scheme provides the conditional probability of non-zero achievable secrecy rate is given by (20), provided at the top of the next page. In (20), we have defined $\Delta J\triangleq(\tilde{\beta}_d+\frac{1}{\tilde{\alpha}_{h,d}})+\frac{1}{\tilde{\alpha}_{g,d}}$. In addition, $\mathbb{X}_{Z_1}$ and $\mathbb{X}_{Z_2}$ are defined in Appendix B.

Proof: Refer to the proof of *Theorem 3*. ∎

Proposition 3: Based on (20), the marginal probability of non-zero achievable secrecy rate achieved by the considered dACDD based PLS system is given by

$$P_r(C_{s,d}>0)=\sum_{d=1}^{M}P_r(C_{s,d}>0|d)P_r(d). \quad (21)$$

Proof: Refer to the proof of *Proposition 2*. ∎

E. Asymptotic diversity gain analysis

We can further simplify (8) as follows:

$$F_{\gamma_{L,d}}(x)=\frac{1}{P_r(d)}\underbrace{\prod_{j=1}^{M}F_{\gamma_{L,j}}(x)}_{J_2} \quad (22)$$

which means that J_2 is same independent of the index of the RRH as for data RRH. In the high SNR region, and over the i.n.i.d. legitimate channels, the corresponding asymptotic expression is given by

$$F_{\gamma_{L,d}}^{\text{as}}(x)=\frac{1}{P_r(d)}\prod_{j=1}^{M}\frac{1}{\Gamma(N_{h,j}+1)}\Big(\frac{x}{\tilde{\alpha}_{h,j}}\Big)^{N_{h,j}}$$
$$=\frac{1}{P_r(d)}\Big(\prod_{j=1}^{M}\frac{1}{\Gamma(N_{h,j}+1)\tilde{\alpha}_{h,j}}\Big)x^{\sum N_h} \quad (23)$$

where $\sum N_h\triangleq\sum_{j=1}^{M}N_{h,j}$.

Based on (23), the asymptotic SOP and probability of non-zero achievable secrecy rate are derived in the following theorem.

Theorem 5: For the i.n.i.d. frequency selective legitimate and eavesdropper channels, the asymptotic conditional SOP and probability of non-zero achievable secrecy rate are respectively given by (24), provided at the top of the next page. In (24), $\mathbb{X}_{P_1}^{\text{as}}$ and $\mathbb{X}_{Z_1}^{\text{as}}$ are defined in Appendix B.

Proof: Refer to the proof of *Theorem 3*. ∎

Proposition 4: When P_J/σ_z^2 is constant [4], the achievable conditional asymptotic SOP by the dth RRH as for the data RRH is given by

$$P_{d,\text{out}}^{\text{as}}(R_s)=\frac{1}{P_r(d)}\prod_{j=1}^{M}\big(\frac{1}{\alpha_{h,j}}\big)^{N_{h,j}}\mathbb{X}_{P_1}^{\text{as}}\big(\frac{P_T}{\sigma_z^2}\big)^{-\sum N_h}$$
$$G_{2,1}^{1,2}\Big(\tilde{\boldsymbol{\beta}}_{g\backslash d}(m_3)\Big|\begin{matrix}1-l_3-N_{g,d},1-l_2-j\\0\end{matrix}\Big) \quad (25)$$

which shows that the achievable diversity gain by the dth RRH when it is selected as the data RRH is given by $G_d=\sum N_h$, independent of the index of the data RRH.

Proof: Refer to the proof of *Proposition 2*. ∎

Proposition 5: When P_J/σ_z^2 is constant, the marginal asymptotic SOP is given by

$$P_{\text{out}}^{\text{as}}(R_s)=\sum_{d=1}^{M}\Big[\prod_{j=1}^{M}\big(\frac{1}{\alpha_{h,j}}\big)^{N_{h,j}}\mathbb{X}_{P_1}^{\text{as}}\big(\frac{P_T}{\sigma_z^2}\big)^{-\sum N_h}$$
$$G_{2,1}^{1,2}\Big(\tilde{\boldsymbol{\beta}}_{g\backslash d}(m_3)\Big|\begin{matrix}1-l_3-N_{g,d},1-l_2-j\\0\end{matrix}\Big)\Big] \quad (26)$$

which shows that the asymptotic diversity gain, G_d, is achievable by the overall system.

IV. Simulation Results

In this section, we first verify the derived closed form expressions for the SOP and probability of non-zero achievable secrecy rate. To this end, we compare the analytically derived performance metric (denoted by **An**) with the perfect performance metric (denoted by **Ex**) for various scenarios. In addition, an asymptotically derived performance metric is denoted by **As**. The corresponding marginal (unconditional) metrics are denoted by **mAn** and **mEx**. Note that mAn SOP and mAn probability of non-zero achievable secrecy rate respectively denote (19) and (21).

$$P_r(C_{s,d}>0|d) = 1-\int_0^{\infty} F_{\gamma_{L,d}}(x) f_{\gamma_{E,d}}(x)dx$$
$$= 1-\frac{1}{P_r(d)}+\frac{\mathbb{X}_{Z_1}}{P_r(d)} G_{2,1}^{1,2}\Big(\frac{\tilde{\boldsymbol{\beta}}_{g\backslash d}(m_3)}{\tilde{\alpha}_{g,d}}\big(\frac{1}{\tilde{\alpha}_{h,d}}-\frac{1}{\tilde{\alpha}_{g,d}}\big)^{-1}\Big|\ \begin{matrix}1-l_1-N_{g,d}, 1-l_2-j\\ 0\end{matrix}\ \Big) -$$
$$\frac{\mathbb{X}_{L_2}}{P_r(d)}\Big[1-\mathbb{X}_{Z_2} G_{2,1}^{1,2}\Big(\frac{\tilde{\boldsymbol{\beta}}_{g\backslash d}(m_3)}{\tilde{\alpha}_{g,d}}(\Delta J)^{-1}\Big|\ \begin{matrix}1-m_2-N_{g,d}, 1-l_2-j\\ 0\end{matrix}\ \Big)\Big]. \tag{20}$$

$$P_{d,\text{out}}^{\text{as}}(R_s) = \frac{1}{P_r(d)}\prod_{j=1}^{M}\big(\frac{1}{\tilde{\alpha}_{h,j}}\big)^{N_{h,j}}\mathbb{X}_{P_1}^{\text{as}} G_{2,1}^{1,2}\Big(\tilde{\boldsymbol{\beta}}_{g\backslash d}(m_3)\Big|\ \begin{matrix}1-l_3-N_{g,d}, 1-l_2-j\\ 0\end{matrix}\ \Big) \text{ and}$$
$$P_r^{\text{as}}(C_{s,d}>0|d) = \frac{1}{P_r(d)}\prod_{j=1}^{M}\big(\frac{1}{\tilde{\alpha}_{h,j}}\big)^{N_{h,j}}\mathbb{X}_{Z_1}^{\text{as}} G_{2,1}^{1,2}\Big(\tilde{\boldsymbol{\beta}}_{g\backslash d}(m_3)\Big|\ \begin{matrix}1-\sum N_h-N_{g,d}, 1-l_2-j\\ 0\end{matrix}\ \Big). \tag{24}$$

- We assume that the LU and EU are respectively placed at $(x=0.5, y=R/2)$ and $(x=1, y=3)$.
- Quadrature phase-shift keying (QPSK) modulation is used. The transmission block size is made of 64 QPSK symbols ($Q=64$). The CP length is given by 16 QPSK symbols ($N_{\text{CP}}=16$). Thus, four RRHs can be used for dACDD operation. As a special performance comparison purpose, we also consider five RRHs. The relative time difference, T_m, between the arrival time of the signal transmitted from RRH_m with respect to RRH_1 is represented as an integer value uniformly generated between 0 and $N_{\text{CP}}=16/4$.
- As for the AIS, we use the ZCS with a size of $Q-1$. One additional zero is added to have the same size as the block data symbol.
- In all scenarios, we fix $P_T=1$ and $R_s=1$. If there are no special remarks, we assume $\rho_J \triangleq P_J/\sigma_z^2 = 2$ dB. A fixed path-loss exponent is assumed to be $\epsilon=2.09$ [38].
- To verify the analytically derived performance metrics, such as the SOP and probability of non-zero achievable secrecy rate, we consider three geometrical scenarios and frequency selective fading channel parameters depending on the locations of the RRHs as follows:

(1) $\mathbb{X}_1$: $M=3$ with three RRHs placed at $\{Re^{j\pi/2}, Re^{j5\pi/6}, Re^{j7\pi/6}\}$.
  (1-a) $\mathbb{X}_{11}: R=5, N_hs=\{1,2,3\}, N_gs=\{3,3,3\}$.
  (1-b) $\mathbb{X}_{12}: R=5, N_hs=\{1,2,3\}, N_gs=\{1,2,3\}$.
  (1-c) $\mathbb{X}_{13}: R=10, N_hs=\{3,2,1\}, N_gs=2$.

(2) $\mathbb{X}_2$: $M=4$ with four RRHs placed at $\{Re^{j\pi/2}, Re^{j3\pi/4}, Re^{j\pi}, Re^{j\pi/4}\}$.
  (2-a) $\mathbb{X}_{21}: R=5, N_hs=\{1,2,3,1\}, N_gs=2$.
  (2-b) $\mathbb{X}_{22}: R=5, N_hs=\{1,2,3,2\}, N_gs=2$.

(3) $\mathbb{X}_3$: $M=5$ with five RRHs are placed at $\{Re^{j\pi/2}, Re^{j3\pi/4}, Re^{j\pi}, Re^{j\pi/4}, Re^{-j\pi/6}\}$.
  (3-a) $\mathbb{X}_{31}: R=5, N_hs=\{1,1,1,1,2\}, N_gs=\{1,2,3,4,1\}$.

(4) When only one element is specified for N_hs and N_gs, this represents that the same number of channel taps is assumed respectively for all legitimate and eavesdropper channels. For example, $N_hs=2$ and $N_gs=2$.

For these scenarios, *Theorem 1* provides the selection probability as follows:

(1-a) : $P_r(d=1)=0.56782$, $P_r(d=2)=0.28957$, and $P_r(d=3)=0.14261$.
(1-b) : $P_r(d=1)=0.56782$, $P_r(d=2)=0.28957$, and $P_r(d=3)=0.14261$.
(1-c) : $P_r(d=1)=0.963157$, $P_r(d=2)=0.0362237$, and $P_r(d=3)=0.000619299$.
(2-a) : $P_r(d=1)=0.40475$, $P_r(d=2)=0.27162$, $P_r(d=3)=0.11599$, and $P_r(d=4)=0.20764$.
(2-b) : $P_r(d=1)=0.302686$, $P_r(d=2)=0.169747$, $P_r(d=3)=0.0583573$, and $P_r(d=4)=0.4692097$.
(3-a) : $P_r(d=1)=0.5009$, $P_r(d=2)=0.1207$, $P_r(d=3)=0.0231$, $P_r(d=4)=0.2812$, and $P_r(d=5)=0.0740$.

These probabilities are also verified numerically.

A. Verification of analytically derived SOP and probability of non-zero achievable secrecy rate

From Fig. 3, we first verify the accuracy of the analytically derived marginal SOP for simulation scenarios $\mathbb{X}_1$ and $\mathbb{X}_2$. For various large and small-scale fading channel parameters, Eqs. (18) and (19) provide a highly reliable accuracy. Thus, without further providing the performance comparisons of the exact SOP with that of analytically derived SOP, we will mainly use the analytically derived SOP in the sequel.

From Fig. 4, we can also verify the accuracy of the analytically derived probability of non-zero achievable secrecy rate for various scenarios. Due to a highly reliable accuracy level, we will mainly use the analytically derived probability of non-zero achievable secrecy rate defined by Eqs. (20) and (21) in the sequel.

B. Secrecy outage probability

For various simulation scenarios, we provide the SOP of the proposed dACDD-based PLS scheme. In generating Fig. 5, we

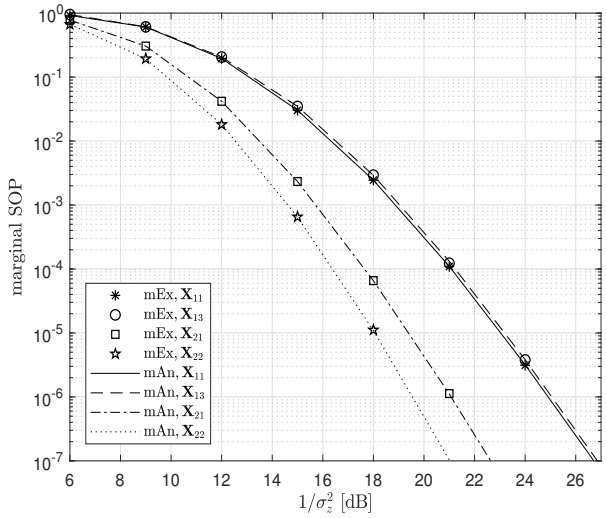

Fig. 3. Marginal SOP for simulation scenarios $\mathbb{X}_1$ and $\mathbb{X}_2$.

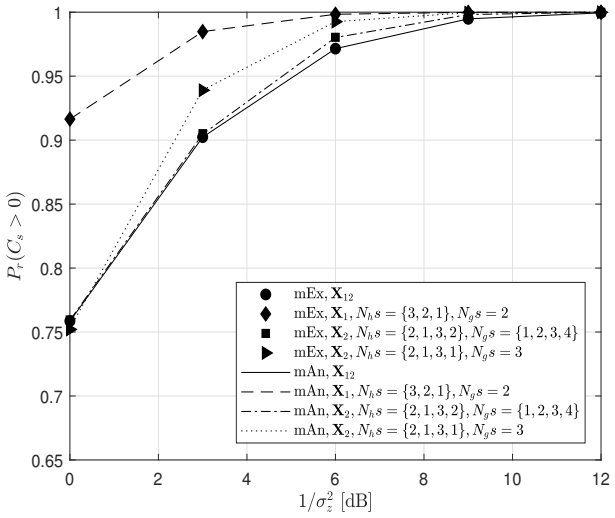

Fig. 4. Marginal probability of non-zero achievable secrecy rate for various simulation scenarios $\mathbb{X}_1$ and $\mathbb{X}_2$. At a fixed $R = 5$, various small-scale fading is considered.

assume that $\sum_{m=1}^{M} N_{h,m} = 4$ and $N_g s = 3$ for scenarios $\mathbb{X}_1$ and $\mathbb{X}_2$. Primary interest of this simulation is to investigate the effect of the sum of the multipath components over the LU channels on the slope of the performance curve of the marginal SOP.

1) When $\sum_{m=1}^{M} N_{h,m}$ is the same, almost the same slope can be obtained in the high SNR region. For example, different combinations for the set $\{N_{h,m}\}$, $\{1,2,1\},\{1,1,2\},\{2,1,1\}$ with three RRHs, and $\{1,1,1,1\}$ with four RRHs, result in the same slope.
2) When a less number of multipath components exists over the eavesdropper channels, a lower marginal SOP can be achieved. For example, N_gs=2 and N_gs=3 for scenario $\mathbb{X}_1$ and $N_h s = \{1,1,2\}$.

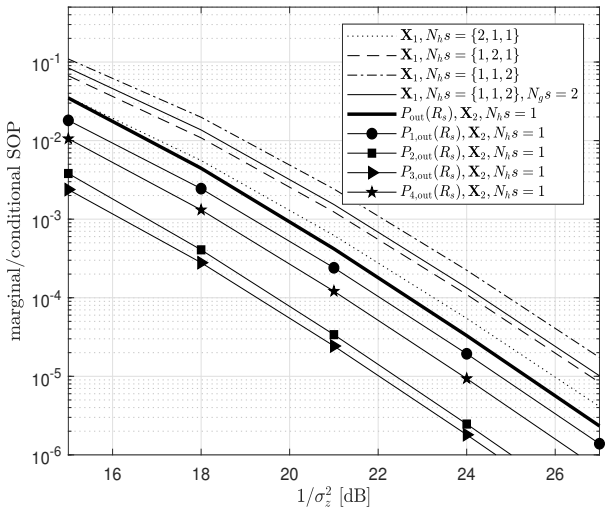

Fig. 5. Exact marginal and conditional SOPs for various scenarios with the constraint of N_gs=3, $\sum_{m=1}^{M} N_{h,m} = 4$, and $R = 5$. Especially, for scenario $\mathbb{X}_2$, $P_{\text{out}}(R_s) = \sum_{d=1}^{4} P_{d,\text{out}}(R_s) P_r(d)$.

3) Due to i.n.i.d frequency selective fading for the legitimate and eavesdropper channels, a different SOP is obtained depending on which RRH is selected as for the data RRH, while maintaining the same slope in the high SNR region. In addition, we can see that the worst conditional SOP, $P_{d,\text{out}}(R_s)$, has a strong effect on the marginal SOP.

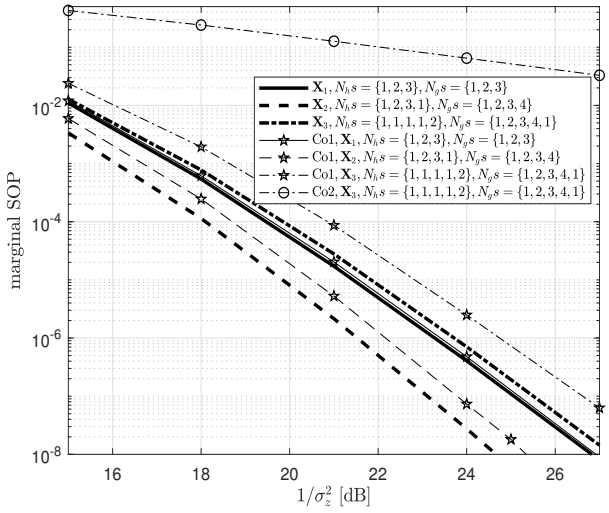

Fig. 6. Marginal SOP for various scenarios with $R = 5$.

In Fig. 6, we compare the marginal SOP of the proposed selection scheme with the conventional selection schemes, denoted by **Co1** and **Co2**, which are explained as follows:

- Co1: Choose one random RRH as the interfering RRH and assign the remaining RRHs as data RRHs, which was proposed in [12].
- Co2: Choose two random RRHs as data and interfering RRHs, which was proposed in [7] and [25].

For various scenarios, this figure shows that as the number of RRHs increases, the performance gap between these two schemes increases, which verifies that the proposed selection will increase PLS as the number of RRHs increases when these RRHs are supported by dACDD. Especially, a significant improvement in the SOP can be achieved over the Co2-based selection scheme. This can be possible by ISI-free reception at the LU. As the number of RRHs increases, the ratio SNR/SINR increases, so that we can have this improvement in the marginal SOP.

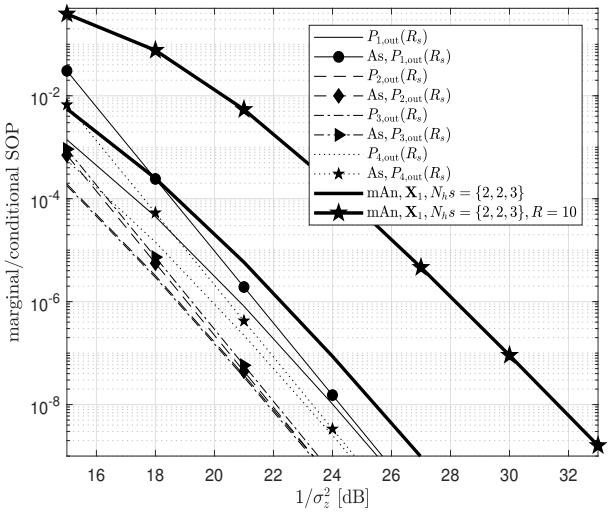

Fig. 7. Marginal and conditional SOPs for various scenarios with $\sum_{m=1}^{M} N_{h,m} = 7$ and either $R = 5$ or $R = 10$.

In Fig. 7, we mainly investigate the diversity gain in the high SNR region. Fig. 5 is also used to summarize the following facts.

- As was verified by propositions 4 and 5, the slopes for $P_{d,\text{out}}(R_s)$ and $P_{\text{out}}(R_s)$ will be the same as $1/\sigma_z^2$ increases. Especially, as $1/\sigma_z^2$ increases, we can see that the diversity gain equals the sum of the multipath components over the legitimate channels by measuring the slope of them. As $1/\sigma_z^2$ increases, the difference between the exact SOP and the asymptotic SOP becomes negligible for the considered scenarios. Comparing with the asymptotic SOP, we can see effects of the small-scale fading on the diversity gain. Note that since the data RRH is selected based on the instantaneous legitimate channel which has the greatest channel magnitude [39], the proposed selection scheme can guarantee that $P_{d,\text{out}}(R_s)$ and $P_{\text{out}}(R_s)$ achieve the same diversity gain even from i.n.i.d. frequency selective fading channels. At the same value of $1/\sigma_z^2$, comparing with the small scale fading used in generating Fig. 5, a lower SOP is obtained due to a greater multipath diversity gain. Thus, as in the general CP-SC systems [39], the proposed dACDD can provide the multiuser and multipath diversity gains simultaneously.
- The sum of the multipath components over the eavesdropper channels has no effect on the diversity gain.
- The distance from the RRHs to the LU and EU, i.e., the large-scale fading, has no effect on the diversity gain. For example, see $R = 5$ vs. $R = 10$ for scenario $\mathbb{X}_1$ with $N_h s = \{2,2,3\}$ and $N_g s = 2$.

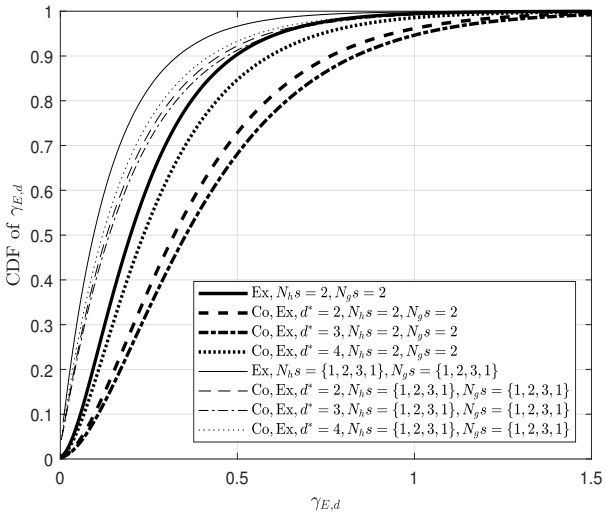

Fig. 8. CDF of the $\gamma_{E,d}$.

As a support of security enhancement by the proposed joint selection of the data and interfering RRHs, we provide Fig. 8 which shows the CDF of $\gamma_{E,d}$ defined by (12). In this simulation, we assume $M = 4$, with $d = 1$ for the data RRH, $R = 5$, $P_T/\sigma_z^2 = 18$ dB, and $\mathbb{X}_2$ scenario. We consider two small-scale fading, i.e., $(N_h s = 2, N_g s = 2)$ and $(N_h s = N_g s = \{1,2,3,1\})$. The conventional selection is assumed to assign only one d^*th RRH as the interfering RRH with $d^* \in \{2,3,4\}$. This figure shows that the proposed joint selection based on dACDD can reduce much more conditional SINR at the EU than the conventional scheme, which results in secrecy enhancement of the considered dACDD-based CP-SC system.

C. Probability of non-zero achievable secrecy rate

In Fig. 9, we mainly investigate the conditional probability of non-zero achievable secrecy rate of the proposed secrecy system with the proposed joint selection for data and interfering RRHs. For three geometrical scenarios, we only consider the first three RRHs for the comparisons. In this simulation, we assume that N_hs=1 for all the cases, and $N_g s = \{1,2,3\}$ for $\mathbb{X}_1$, $N_g s = \{1,2,3,4\}$ for $\mathbb{X}_2$, and $N_g s = \{1,2,3,4,1\}$ for $\mathbb{X}_3$. This figure shows the following facts.

- A less $1/\sigma_z^2$ is required to achieve the same level of probability of non-zero achievable secrecy rate as the number of RRHs increases.
- As a specific example, when N_hs=1 for all the legitimate channels, $\sum_{m=1}^{M} N_{h,m}$ increases as the number of RRH increases. Thus, as the number of RRHs increases, it converges more quickly to one.
- Each RRH results in a different SINR at the EU due to i.n.i.d. fading channels, so that a different value of P_T/σ_z^2

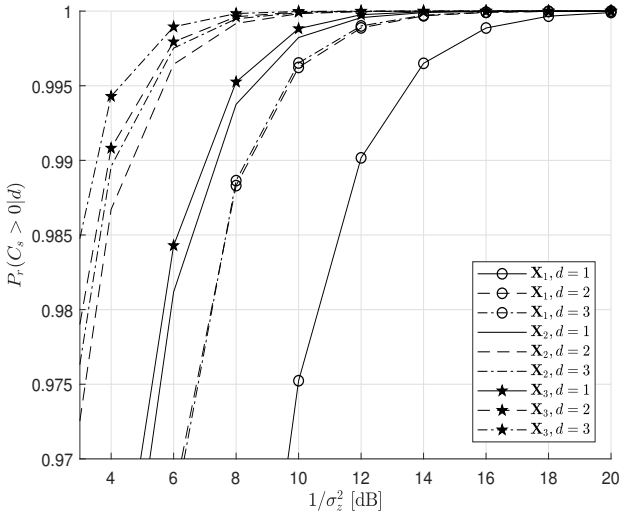

Fig. 9. Conditional probability of non-zero achievable secrecy rate for various scenarios with N_hs=1 and $R = 5$.

is required to achieve a particular probability of non-zero achievable secrecy rate.

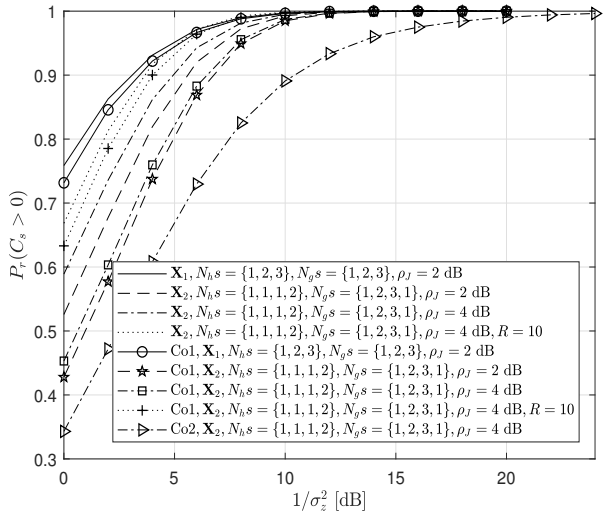

Fig. 10. Marginal probability of non-zero achievable secrecy rate for various scenarios with either $R = 5$ or $R = 10$.

In Fig. 10, we compare the marginal probability of non-zero achievable secrecy rate of the system with the proposed joint selection for data and interfering RRHs with that of the conventional selection scheme under the framework of dACDD, which chooses one data RRH and one interfering RRH. This figure shows the following facts.

- As $\sum_{m=1}^{M} N_{h,m}$ increases, a faster convergence time is obtained in achieving a desired probability.
- As the number of RRHs increases, a bigger performance improvement can be achieved due to a decreased SINR at the EU. In the considered scenarios, the number of RRHs has much influence on the performance than the number of multipath components.
- As ρ_J increases, a performance improvement can be achieved due to a much decreased SINR at the EU. For example, $\rho_J = 2$ dB vs. $\rho_J = 4$ dB for scenario $\mathbb{X}_2$, $N_h s = \{1,1,1,2\}$, $N_g s = \{1,2,3,1\}$, and $R = 5$.
- As the distance from the RRHs to the LU and EU increases, the large scale fading factor becomes smaller, so that the benefit of decreasing SINR at the EU will be reduced by using more interfering RRHs, while the proposed selection scheme still results in a higher marginal probability of non-zero achievable secrecy rate over the conventional one.
- Especially, comparing with the convectional Co2 scheme, a significant improvement can be obtained for the marginal probability of non-zero achievable secrecy rate.

V. Conclusions

In this paper, we have proposed a new transmit diversity scheme, dACDD, which provides the maximum diversity gain even for asynchronous reception at a legitimate user. Under the framework of this dACDD, a joint selection scheme for the data RRH and interfering RRHs has been developed to achieve a higher PLS. Since perfect CSI of the whole legitimate and eavesdropper channels is not available at the transmitting side, we have proposed this scheme, which exploits the maximum achievable diversity gain, while minimizing the SINR at an eavesdropping user. For i.n.i.d. frequency selective legitimate and eavesdropper channels, new closed-form expressions for the selection probability of the RRH as for the data RRH, SOP, and probability of non-zero achievable secrecy rate have been derived. Their accuracy have been also verified by the link-level simulations. In the high SNR regions, the achievable diversity gain has been shown to be the sum of the number of multipath components over the legitimate channels, independent of the index of the RRH specifying the data RRH and the large-scale fading. Compared with the conventional two selection schemes for the data RRH and interfering RRH, the proposed selection scheme has been shown to achieve better performance as the number of RRHs increases.

Appendix A: Derivation of Theorem 1

We can compute $P_r(d)$ as follows:

$$\begin{aligned} P_r(d) = \int_0^\infty & P_r(\gamma_{L,1} < x | \gamma_{L,d} = x) \cdots \\ & P_r(\gamma_{L,d-1} < x | \gamma_{L,d} = x) P_r(\gamma_{L,d+1} < x | \gamma_{L,d} = x) \cdots \\ & P_r(\gamma_{L,M} < x | \gamma_{L,d} = x) f_{\gamma_{L,d}}(x) dx \\ = \int_0^\infty & f_{\gamma_{L,d}}(x) \prod_{j=1, j\neq d}^{M} F_{\gamma_{L,j}}(x) dx. \end{aligned} \tag{A.1}$$

For the i.n.i.d. frequency selective LU channels, $\prod_{j=1, j\neq d}^{M} F_{\gamma_{L,j}}(x)$ is given by

$$\prod_{j=1, j\neq d}^{M} F_{\gamma_{L,j}}(x) = 1 + \sum_{m=1}^{M-1} (-1)^m \Upsilon_d \prod_{t=1}^{m} \Big(\frac{1}{\ell_t! (\tilde{\boldsymbol{\beta}}_{h\setminus d}(q_t))^{\ell_t}} \Big)$$

$$e^{-\tilde{\beta}_d x} x^{\tilde{l}_d}. \tag{A.2}$$

In addition, the PDF of the RV $\gamma_{L,d}$ is given by

$$f_{\gamma_{L,d}}(x) = \frac{1}{\Gamma(N_{h,d})(\tilde{\alpha}_{h,d})^{N_{h,d}}} e^{-\frac{x}{\tilde{\alpha}_{h,d}}} (x)^{N_{h,d}-1}. \tag{A.3}$$

Having applied (A.3) to (A.1), we can have

$$\begin{aligned} P_r(d) &= 1 + \frac{1}{\Gamma(N_{h,d})(\tilde{\alpha}_{h,d})^{N_{h,d}}} \sum_{m=1}^{M-1} (-1)^m \Upsilon_d \\ &\prod_{t=1}^{m} \Big(\frac{1}{\ell_t! (\tilde{\boldsymbol{\beta}}_{h\setminus d}(q_t))^{\ell_t}} \Big) \int_0^{\infty} e^{-(\tilde{\beta}_d + \frac{1}{\tilde{\alpha}_{h,d}})x} x^{N_{h,d}+\tilde{l}_d-1} dx \\ &= 1 + \frac{1}{\Gamma(N_{h,d})(\tilde{\alpha}_{h,d})^{N_{h,d}}} \sum_{m=1}^{M-1} (-1)^m \Upsilon_d \Gamma(N_{h,d}+\tilde{l}_d) \\ &\prod_{t=1}^{m} \Big(\frac{1}{\ell_t! (\tilde{\boldsymbol{\beta}}_{h\setminus d}(q_t))^{\ell_t}} \Big) \big(\tilde{\beta}_d + \frac{1}{\tilde{\alpha}_{h,d}} \big)^{-(N_{h,d}+\tilde{l}_d)}. \end{aligned} \tag{A.4}$$

Appendix B: Several Definitions

$\mathbb{X}_{L_2}, \mathbb{X}_E, \mathbb{X}_{P_1}, \mathbb{X}_{P_2}, \mathbb{X}_{Z_1}, \mathbb{X}_{Z_2}, \mathbb{X}_{P_1}^{\text{as}}$, and $\mathbb{X}_{Z_1}^{\text{as}}$ are defined in (B.1), provided at the top of the next page.

Appendix C: Derivation of Theorem 2

The PDF of the RV A is given by

$$f_A(x) = \frac{x^{N_{g,d}-1}}{\Gamma(N_{g,d})(\tilde{\alpha}_{g,d})^{N_{g,d}}} e^{-\frac{x}{\alpha_{g,d}}}. \tag{C.1}$$

Moreover, the PDF of the RV B is given by

$$\begin{aligned} f_B(x) = &\sum_{m_3=1, m_3\neq d}^{M} \sum_{j=1}^{N_{g,m_3}} \frac{(-1)^{m_3} \boldsymbol{\theta}_{m_3\setminus d}(j)}{\Gamma(j)} x^{j-1} \\ &e^{-\frac{x}{\tilde{\boldsymbol{\beta}}_{g\setminus d}(m_3)}} \end{aligned} \tag{C.2}$$

where the jth element of $\boldsymbol{\theta}_{m_3\setminus d}$ is defined by

$$\begin{aligned} \boldsymbol{\theta}_{m_3\setminus d}(j) \triangleq & \frac{(-1)^{N_{g,m_3}}}{(\tilde{\boldsymbol{\beta}}_{g\setminus d}(m_3))^{N_{g,m_3}}} \sum_{\mathbb{S}(m_3,j)} \prod_{k=1,k\neq m_3}^{M-1} \binom{\bar{N}_{g,k}}{q_k} \\ & \frac{(\tilde{\boldsymbol{\beta}}_{g\setminus d}(k))^{q_k}}{(1 - \frac{\tilde{\boldsymbol{\beta}}_{g\setminus d}(k)}{\tilde{\boldsymbol{\beta}}_{g\setminus d}(m_3)})^{N_{g,k}+q_k}} \end{aligned}$$

with $\bar{N}_{g,k} \triangleq N_{g,k} + q_k - 1$ and $\mathbb{S}(i,j)$ is a set of $(M-1)$-tuples satisfying the following condition

$$\mathbb{S}(i,j) \triangleq \{(q_1, \ldots, q_{M-1}) : \sum_{k=1}^{M-1} q_k = N_{g,i} - j \text{ with } q_i = 0\}.$$

Now the PDF of the RV $\gamma_{E,d}$ is given by (C.3), provided at the bottom of the next page.

Appendix D: Derivation of Theorem 3

From (10), we first compute

$$\begin{aligned} F_{\gamma_{L,d}}(J_R(1+x)-1) = &\frac{1}{P_r(d)} - \frac{\mathbb{X}_{L_1}}{P_r(d)} e^{-\frac{(J_R-1)}{\tilde{\alpha}_{h,d}}} \\ &\sum_{j_2=0}^{l_1} \binom{l_1}{j_2} (J_R-1)^{l_1-j_2} x^{j_2} e^{-\frac{J_R}{\tilde{\alpha}_{h,d}}x} + \frac{\mathbb{X}_{L_2}}{P_r(d)} \\ &\Big(1 - e^{-(J_R-1)(\tilde{\beta}_d + \frac{1}{\tilde{\alpha}_{h,d}})} \sum_{m_2=0}^{N_{h,d}+\tilde{l}_d-1} \frac{\big(\tilde{\beta}_d + \frac{1}{\tilde{\alpha}_{h,d}}\big)^{m_2}}{\Gamma(m_2+1)} \\ &\sum_{j_2=0}^{m_2} \binom{m_2}{j_2} (J_R-1)^{m_2-j_2} x^{j_2} e^{-J_R(\tilde{\beta}_d + \frac{1}{\tilde{\alpha}_{h,d}})x} \Big). \end{aligned} \tag{D.1}$$

Using (D.1), the two key parts of the SOP are evaluated as (D.2), provided at the bottom of the next page. From (D.2), we can derive (18).

References

[1] K. J. Kim, H. Liu, M. Wen, P. V. Orlik, and H. V. Poor, "Distributed asynchronous CDD-based cooperative systems with a passive eavesdropper," in *Proc. IEEE Global Commun. Conf.*, Waikoloa, HI, Dec. 2019, pp. 1–6.

[2] L. Dong, Z. Han, A. P. Petropulu, and H. V. Poor, "Improving wireless physical layer security via cooperative relays," *IEEE Trans. Signal Process.*, vol. 58, no. 3, pp. 1875–1888, Mar. 2010.

[3] N. Yang, P. L. Yeoh, M. Elkashlan, R. Schober, and I. B. Collings, "Transmit antenna selection for security enhancement in MIMO wiretap channels," *IEEE Trans. Commun.*, vol. 61, no. 1, pp. 144–154, Jan. 2013.

[4] L. Wang, K. J. Kim, T. Q. Duong, M. Elkashlan, and H. V. Poor, "Security enhancement of cooperative single carrier systems," *IEEE Trans. Inf. Forensics Security*, vol. 10, no. 1, pp. 90–103, Jan. 2015.

[5] F. Al-Qahtani, C. Zhong, and H. Ainuweiri, "Opportunistic relay selection for secrecy enhancement in cooperative networks," *IEEE Trans. Commun.*, vol. 63, pp. 1756–1770, May 2015.

[6] K. J. Kim, P. L. Yeoh, P. Orlik, and H. V. Poor, "Secrecy performance of finite-sized cooperative single carrier systems with unreliable backhaul connections," *IEEE Trans. Signal Process.*, vol. 64, no. 17, pp. 4403–4416, Sep. 2016.

[7] Y. Zou, "Physical-layer security for spectrum sharing systems," *IEEE Trans. Wireless Commun.*, vol. 16, no. 2, pp. 1319–1329, Feb. 2017.

[8] G. Goel and R. Negi, "Guaranteeing secrecy using artificial noise," *IEEE Trans. Wireless Commun.*, vol. 7, no. 6, pp. 2180–2189, Jul. 2008.

[9] I. Krikidis, J. S. Thompson, and S. Mclaughlin, "Relay selection for secure cooperative networks with jamming," *IEEE Trans. Wireless Commun.*, vol. 8, no. 10, pp. 5003–5011, Oct. 2009.

[10] A. S. Khan and I. Chatzigeorgiou, "Opportunistic relaying and random linear network coding for secure and reliable communication," *IEEE Trans. Wireless Commun.*, vol. 17, no. 1, pp. 223–234, Jan. 2018.

[11] L. Hu, H. Wen, B. Wu, J. Tang, F. Pan, and R. Liao, "Cooperative-jamming-aided secrecy enhancement in wireless networks with passive eavesdroppers," *IEEE Trans. Veh. Technol.*, vol. 67, no. 3, pp. 2108–2117, Mar. 2018.

[12] K. J. Kim, H. Liu, M. D. Renzo, P. V. Orlik, and H. V. Poor, "Secrecy analysis of distributed CDD-based cooperative systems with deliberate interference," *IEEE Trans. Wireless Commun.*, vol. 17, no. 12, pp. 7865 – 7878, Dec. 2018.

[13] X. Zhou and M. R. McKay, "Secure transmission with artificial noise over fading channels: Achievable rate and optimal power allocation," *IEEE Trans. Veh. Technol.*, vol. 59, no. 8, pp. 3831–3842, Oct. 2010.

[14] C. Wang and H. Wang, "Robust joint beamforming and jamming for secure AF networks: Low-complexity design," *IEEE Trans. Veh. Technol.*, vol. 64, no. 5, pp. 2192–2198, May 2015.

[15] H. Wang, C. Wang, and D. W. K. Ng, "Artificial noise assisted secure transmission under training and feedback," *IEEE Trans. Signal Process.*, vol. 63, no. 23, pp. 6285–6298, Dec. 2015.

[16] H. Wang, M. Luo, X. Xia, and Q. Yin, "Joint cooperative beamforming and jamming to secure AF relay systems with individual power constraint and no eavesdropper's CSI," *IEEE Signal Process. Lett.*, vol. 20, no. 1, pp. 39–42, Jan. 2013.

$$\mathbb{X}_{L_2}\triangleq\big(\tilde{\beta}_d+\frac{1}{\tilde{\alpha}_{h,d}}\big)^{-(N_{h,d}+\tilde{l}_d)}\frac{\Gamma(N_{h,d}+\tilde{l}_d)}{\Gamma(N_{h,d})(\tilde{\alpha}_{h,d})^{N_{h,d}}}\sum_{m_1=1}^{M-1}(-1)^{m_1}\Upsilon_d\prod_{t=1}^{m_1}\Big(\frac{1}{\ell_t!(\tilde{\boldsymbol{\beta}}_{h\backslash d}(q_t))^{\ell_t}}\Big),$$

$$\mathbb{X}_E\triangleq\frac{1}{\Gamma(N_{g,d})(\tilde{\alpha}_{g,d})^{N_{g,d}}}\sum_{m_3=1,m_3\neq d}^{M}\sum_{j=1}^{N_{g,m_3}}\sum_{l_2=0}^{N_{g,d}}\frac{(-1)^{m_3}\boldsymbol{\theta}_{m_3\backslash d}(j)}{\Gamma(j)}\binom{N_{g,d}}{l_2}\Gamma(l_2+j),$$

$$\mathbb{X}_{P_1}\triangleq\mathbb{X}_{L_1}e^{-\frac{(J_R-1)}{\tilde{\alpha}_{h,d}}}\sum_{j_2=0}^{l_1}\binom{l_1}{j_2}\mathbb{X}_E\big(\frac{1}{\tilde{\boldsymbol{\beta}}_{g\backslash d}(m_3)}\big)^{-l_2-j}\frac{(J_R-1)^{l_1-j_2}J_R^{j_2}}{\Gamma(l_2+j)}\big(\frac{J_R}{\tilde{\alpha}_{h,d}}+\frac{1}{\tilde{\alpha}_{g,d}}\big)^{-j_2-N_{g,d}},$$

$$\mathbb{X}_{P_2}\triangleq e^{-(J_R-1)(\tilde{\beta}_d+\frac{1}{\tilde{\alpha}_{h,d}})}\sum_{m_2=0}^{N_{h,d}+\tilde{l}_d-1}\frac{1}{\Gamma(m_2+1)}\big(\tilde{\beta}_d+\frac{1}{\tilde{\alpha}_{h,d}}\big)^{m_2}\sum_{j_3=0}^{m_2}\binom{m_2}{j_3}(J_R-1)^{m_2-j_3}(J_R)^{j_3}$$
$$\mathbb{X}_E\big(\frac{1}{\tilde{\boldsymbol{\beta}}_{g\backslash d}(m_3)}\big)^{-l_2-j}\frac{1}{\Gamma(l_2+j)}\big(J_R(\tilde{\beta}_d+\frac{1}{\tilde{\alpha}_{h,d}})+\frac{1}{\tilde{\alpha}_{g,d}}\big)^{-j_3-N_{g,d}},$$

$$\mathbb{X}_{Z_1}\triangleq\mathbb{X}_{L_1}\mathbb{X}_E\big(\frac{1}{\tilde{\boldsymbol{\beta}}_{g\backslash d}(m_3)}\big)^{-l_2-j}\frac{1}{\Gamma(l_2+j)}\big(\frac{1}{\tilde{\alpha}_{h,d}}+\frac{1}{\tilde{\alpha}_{g,d}}\big)^{-l_1-N_{g,d}},$$

$$\mathbb{X}_{Z_2}\triangleq\sum_{m_2=0}^{N_{h,d}+\tilde{l}_d-1}\frac{1}{\Gamma(m_2+1)}\big(\tilde{\beta}_d+\frac{1}{\tilde{\alpha}_{h,d}}\big)^{m_2}\mathbb{X}_E\big(\frac{1}{\tilde{\boldsymbol{\beta}}_{g\backslash d}(m_3)}\big)^{-l_2-j}\frac{1}{\Gamma(l_2+j)}\big((\tilde{\beta}_d+\frac{1}{\tilde{\alpha}_{h,d}})+\frac{1}{\tilde{\alpha}_{g,d}}\big)^{-m_2-N_{g,d}},$$

$$\mathbb{X}_{Z_1}^{\text{as}}\triangleq\Big(\prod_{j\in\mathbb{S}_M}\frac{1}{\Gamma(N_{h,j}+1)}\Big)\mathbb{X}_E\big(\frac{1}{\tilde{\boldsymbol{\beta}}_{g\backslash d}(m_3)}\big)^{-l_2-j}\frac{1}{\Gamma(l_2+j)}\big(\frac{1}{\tilde{\alpha}_{g,d}}\big)^{-\sum N_h-N_{g,d}},\text{ and}$$

$$\mathbb{X}_{P_1}^{\text{as}}\triangleq\Big(\prod_{j\in\mathbb{S}_M}\frac{1}{\Gamma(N_{h,j}+1)}\Big)\mathbb{X}_E\sum_{l_3=0}^{\sum N_h}\binom{\sum N_h}{l_3}(J_R-1)^{(\sum N_h-l_3)}(J_R)^{l_3}\big(\frac{1}{\tilde{\beta}_{g,m_3,\backslash d}}\big)^{-l_2-j}\frac{1}{\Gamma(l_2+j)}\big(\frac{1}{\tilde{\alpha}_{g,d}}\big)^{-l_3-N_{g,d}}.\quad\text{(B.1)}$$

$$\begin{aligned}f_{\gamma_{E,d}}(x)&=\int_0^\infty(t+1)f_A((t+1)x)f_B(t)dt\propto\int_0^\infty(t+1)\big((t+1)x\big)^{N_{g,d}-1}e^{-\frac{(t+1)x}{\tilde{\alpha}_{g,d}}}t^{j-1}e^{-\frac{x}{\tilde{\boldsymbol{\beta}}_{g\backslash d}(m)}}dt\\&=e^{-\frac{x}{\tilde{\alpha}_{g,d}}}(x)^{N_{g,d}-1}\sum_{l=0}^{N_{g,d}}\binom{N_{g,d}}{l}\int_0^\infty t^{l+j-1}e^{-t\left(\frac{x}{\tilde{\alpha}_{g,d}}+\frac{1}{\tilde{\boldsymbol{\beta}}_{g\backslash d}(m)}\right)}dt\\&=e^{-\frac{x}{\tilde{\alpha}_{g,d}}}(x)^{N_{g,d}-1}\sum_{l=0}^{N_{g,d}}\binom{N_{g,d}}{l}\Gamma(l+j)\big(\frac{x}{\tilde{\alpha}_{g,d}}+\frac{1}{\tilde{\boldsymbol{\beta}}_{g\backslash d}(m)}\big)^{-(l+j)}.\end{aligned}\quad\text{(C.3)}$$

$$\begin{aligned}P_{d,\text{out},1}(R_s)&\propto\mathbb{X}_E\int_0^\infty x^{j_2+N_{g,d}-1}e^{-x(\frac{J_R}{\tilde{\alpha}_{h,d}}+\frac{1}{\tilde{\alpha}_{g,d}})}\big(\frac{x}{\tilde{\alpha}_{g,d}}+\frac{1}{\tilde{\boldsymbol{\beta}}_{g\backslash d}(m_3)}\big)^{-(l_2+j)}\\&=\mathbb{X}_E\big(\frac{1}{\tilde{\boldsymbol{\beta}}_{g\backslash d}(m_3)}\big)^{-l_2-j}\frac{1}{\Gamma(l_2+j)}\big(\frac{J_R}{\tilde{\alpha}_{h,d}}+\frac{1}{\tilde{\alpha}_{g,d}}\big)^{-j_2-N_{g,d}}\\&\quad G_{2,1}^{1,2}\Big(\frac{\tilde{\boldsymbol{\beta}}_{g\backslash d}(m_3)}{\tilde{\alpha}_{g,d}}\big(\frac{J_R}{\tilde{\alpha}_{h,d}}+\frac{1}{\tilde{\alpha}_{g,d}}\big)^{-1}\Big|\begin{matrix}1-j_2-N_{g,d},1-l_2-j\\0\end{matrix}\Big),\text{ and}\\P_{d,\text{out},2}(R_s)&\propto\mathbb{X}_E\int_0^\infty x^{j_3+N_{g,d}-1}e^{-x(J_R(\tilde{\beta}_d+\frac{1}{\tilde{\alpha}_{h,d}})+\frac{1}{\tilde{\alpha}_{g,d}})}\big(\frac{x}{\tilde{\alpha}_{g,d}}+\frac{1}{\tilde{\boldsymbol{\beta}}_{g\backslash d}(m_3)}\big)^{-(l_2+j)}\\&=\mathbb{X}_E\big(\frac{1}{\tilde{\boldsymbol{\beta}}_{g\backslash d}(m_3)}\big)^{-l_2-j}\frac{1}{\Gamma(l_2+j)}\big(J_R(\tilde{\beta}_d+\frac{1}{\tilde{\alpha}_{h,d}})+\frac{1}{\tilde{\alpha}_{g,d}}\big)^{-j_3-N_{g,d}}\\&\quad G_{2,1}^{1,2}\Big(\frac{\tilde{\boldsymbol{\beta}}_{g\backslash d}(m_3)}{\tilde{\alpha}_{g,d}}\big(J_R(\tilde{\beta}_d+\frac{1}{\tilde{\alpha}_{h,d}})+\frac{1}{\tilde{\alpha}_{g,d}}\big)^{-1}\Big|\begin{matrix}1-j_3-N_{g,d},1-l_2-j\\0\end{matrix}\Big).\end{aligned}\quad\text{(D.2)}$$

---

[17] L. Wang, Y. Cai, Y. Zou, W. Yang, and L. Hanzo, "Joint relay and jammer selection improves the physical layer security in the face of CSI feedback delays," *IEEE Trans. Veh. Technol.*, vol. 65, no. 8, pp. 6259–6274, Aug. 2016.

[18] K. Wang, L. Yuan, T. Miyazaki, S. Guo, and Y. Sun, "Antieavesdropping with selfish jamming in wireless networks: A bertrand game approach," *IEEE Trans. Veh. Technol.*, vol. 66, no. 7, pp. 6268–6279, Jul. 2017.

[19] B. Clerckx, G. Kim, J. Choi, and Y.-J. Hong, "Elicit vs. implicit feedback for SU and MU-MIMO," in *Proc. IEEE Global Commun. Conf.*, Miami, FL, Dec. 2010, pp. 1–5.

[20] K. J. Kim, M. D. Renzo, H. Liu, P. V. Orlik, and H. V. Poor, "Performance analysis of distributed single carrier systems with distributed cyclic delay diversity," *IEEE Trans. Commun.*, vol. 65, no. 12, pp. 5514–5528, Dec. 2017.

[21] K. J. Kim, H. Liu, M. Wen, M. D. Renzo, and H. V. Poor, "Outage probability analysis of spectrum sharing systems with distributed cyclic delay diversity," *IEEE Trans. Commun.*, vol. 67, no. 6, pp. 4435–4449, Jun. 2019.

[22] K. J. Kim and T. A. Tsiftsis, "Performance analysis of QRD-based cyclically prefixed single-carrier transmissions with opportunistic scheduling," *IEEE Trans. Veh. Technol.*, vol. 60, pp. 328–333, Jan. 2011.

[23] H. Wang, C. Wang, D. W. K. Ng, M. H. Lee, and J. Xiao, "Artificial noise assisted secure transmission for distributed antenna systems," *IEEE Trans. Signal Process.*, vol. 64, no. 15, pp. 4050–4064, Aug. 2016.

[24] H. Wang, "Full-diversity uncoordinated cooperative transmission for asynchronous relay networks," *IEEE Trans. Veh. Technol.*, vol. 66, no. 1, pp. 1939–9359, Jan. 2017.

[25] G. Wu, Q. Du, and K. Hua, "Selective random CDD enhanced joint cooperative relay and HARQ for delay-tolerant vehicular communications," *International Journal of Distributed Sensor Networks*, vol. 11, no. 5, pp. 1–11, May 2015.

[26] J. Blumenstein and M. Bobula, "Coarse time synchronization utilizing symmetric properties of Zadoff Chu sequences," *IEEE Commun. Lett.*, vol. 22, no. 5, pp. 1006–1009, May 2018.

[27] K. Lee, J. Kim, J. Jung, and I. Lee, "Zadoff-Chu sequence based signature identification for OFDM," *IEEE Trans. Wireless Commun.*, vol. 12, no. 10, pp. 4932–4942, Oct. 2013.

[28] T. K. Y. Lo, "Maximum ratio transmission," *IEEE Trans. Commun.*, vol. 47, no. 10, pp. 1458–1461, Oct. 1999.

[29] K. J. Kim, T. Khan, and P. Orlik, "Performance analysis of cooperative systems with unreliable backhauls and selection combining," *IEEE Trans. Veh. Technol.*, vol. 66, no. 3, pp. 2448–2461, Mar. 2017.

[30] N. Nguyen, H. Q. Ngo, T. Q. Duong, H. D. Tuan, and K. Tourki, "Secure massive mimo with the artificial noise-aided downlink training," *IEEE J. Sel. Areas Commun.*, vol. 36, no. 4, pp. 802–816, Apr. 2018.

[31] Y. Ju, H. Wang, T. Zheng, and Q. Yin, "Secure transmissions in millimeter wave systems," *IEEE Trans. Commun.*, vol. 65, no. 5, pp. 2114–2127, May 2017.

[32] B. Devillers, J., and L. Vandendorpe, "About the diversity in cyclic prefixed single-carrier systems," *Physical Communication*, vol. 1, no. 4, pp. 266 – 276, 2008.

[33] R. Rajashekar, K. V. S. Hari, and L. Hanzo, "Spatial modulation aided zero-padded single carrier transmission for dispersive channels," *IEEE Trans. Commun.*, vol. 61, no. 6, pp. 2318–2329, Jun. 2013.

[34] L. Deneire, B. Gyselinckx, and M. Engels, "Training sequence versus cyclic prefix-a new look on single carrier communication," *IEEE Commun. Lett.*, vol. 5, no. 7, pp. 292–294, Jul. 2001.

[35] Y. Zeng and T. S. Ng, "Pilot cyclic prefixed single carrier communication: channel estimation and equalization," *IEEE Signal Process. Lett.*, vol. 12, no. 1, pp. 56–59, Jan. 2005.

[36] Y. Hou and T. Hase, "Improvement on the channel estimation of pilot cyclic prefixed single carrier (PCP-SC) system," *IEEE Signal Process. Lett.*, vol. 16, no. 8, pp. 719–722, Aug. 2009.

[37] I. S. Gradshteyn and I. M. Ryzhik, *Table of Integrals, Series, and Products*. New York: Academic Press, 2007.

[38] 3GPP, TR 36.828 (V11.0.0), "Further enhancements to LTE time division duplex (TDD) for downlink-uplink (DL-UL) interference management and traffic adaptation," Jun. 2012.

[39] K. J. Kim and T. A. Tsiftsis, "On the performance of cyclic prefix-based single-carrier cooperative diversity systems with best relay selection," *IEEE Trans. Wireless Commun.*, vol. 10, no. 4, pp. 1269–1279, Apr. 2011.